Toward a Light-Driven Motorized Nanocar: Synthesis and Initial Imaging of Single Molecules

Pinn-Tsong Chiang,[†] Johannes Mielke,[‡] Jazmin Godoy,[†] Jason M. Guerrero,[†] Lawrence B. Alemany,[†] Carlos J. Villagómez,[‡] Alex Saywell,[‡] Leonhard Grill,[‡,*] and James M. Tour[†,*]

[†]Departments of Chemistry and Mechanical Engineering and Materials Science, and the Smalley Institute for Nanoscale Science and Technology, Rice University, Houston, Texas 77005, United States and, [‡]Department of Physical Chemistry, Fritz-Haber-Institut der Max-Planck-Gesellschaft, Faradayweg 4-6, D-14195 Berlin, Germany

ABSTRACT

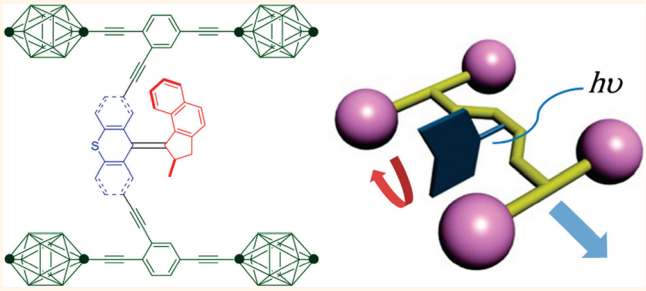

A second generation motorized nanocar was designed, synthesized, and imaged. To verify structural integrity, NMR-based COSY, NOESY, DEPT, HSQC, and HMBC experiments were conducted on the intermediate motor. All signals in ^{1}H NMR were unambiguously assigned, and the results were consistent with the helical structure of the motor. The nanocar was deposited on a Cu(111) surface, and single intact molecules were imaged by scanning tunneling microscopy (STM) at 5.7 K, thereby paving the way for future single-molecule studies of this motorized nanocar atop planar substrates.

KEYWORDS: nanomachine · nanocar · molecular motor scanning tunneling microscopy · metal surface

Organic synthesis has recently been applied to the construction of single-molecule machines. These nanomachines include, for example, switches,[1] shuttles,[2] and muscles[3] that were designed to perform their namesake functions at the molecular level when proper external stimuli are applied. We recently developed a family of nanovehicles termed nanocars[4,5] that were designed to operate on surfaces and to be studied at the single-molecule level. They were imaged by scanning tunneling microscopy (STM) on metallic surfaces[6] and nonconducting glass surfaces using single-molecule fluorescence microscopy (SMFM).[7,8] The ultimate purpose of our research has been to synthesize nanomachines that can transport nanocargo (materials or information) from one place to another on a surface. The first nanocar, which comprised a chassis and two axles mounted with four C_{60} wheels, exemplified structurally controlled directional movement on a surface due to rolling of the wheels.[9,10] The motion could be thermally (heated substrate surface) or electrically (STM-tip field) induced, thus opening the way to molecular-structure-defined motion at the nanoscale. Our next goal was to synthesize a nanomachine that can convert energy input (light or chemically powered)[11] into controlled motion on a surface. Hence, we prepared the first generation motorized nanocar (**1**),[12] intended to harvest light as fuel (Figure 1). In designing nanocar **1**, we replaced the oligo(phenylene ethynylene) (OPE) chassis of the first C_{60}-wheeled nanocar with a light-driven unidirectional molecular motor. Also, we opted for *p*-carborane wheels because C_{60} quenched the photoisomerization process of the molecular motor.[12−14] We intended for the paddle-like rotor to interact with the surface and thereby generate force to propel the nanocar upon irradiation.

The kinetic parameters of the helical inversion process of nanocar **1** in solution, the rate-determining step of the motor rotation, were obtained by proton NMR. The result was similar to the data obtained by Feringa and co-workers for the motor bearing two methoxy groups at the 2- and 7-positions on the thioxanthene stator.[15] These results were encouraging since the relatively bulky *p*-carborane-containing axles did not alter the rotation of the motor. However, the slow rotation of the motor, 202 h for a complete rotation at ambient temperature (1.8 rotations/h at 65 °C),[12] was a problem for surface studies.

Hence, a molecular motor with a lower energy barrier to the rotation process was needed. Feringa and co-workers determined that fine-tuning of the original motor

* Address correspondence to lgr@fhi-berlin.mpg.de, tour@rice.edu.

Received for review October 14, 2011 and accepted November 30, 2011.

Published online November 30, 2011
10.1021/nn203969b

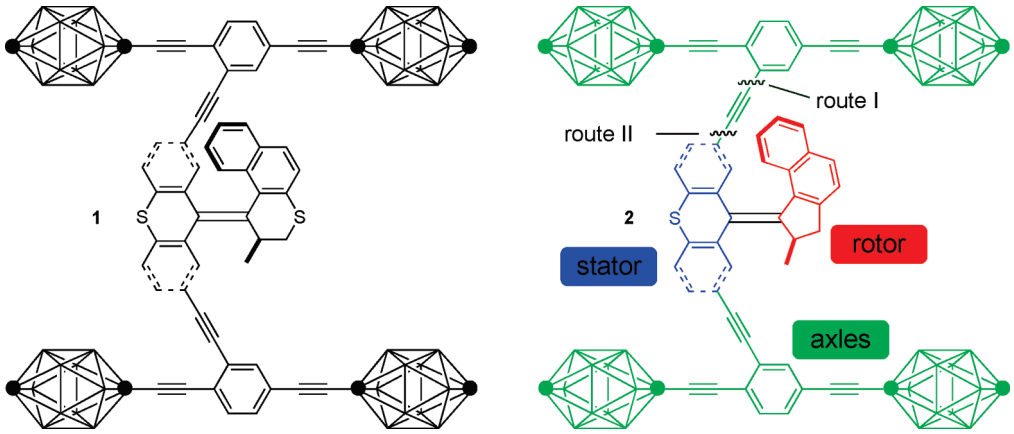

Figure 1. (Left) Structure of first generation motorized nanocar 1. The *p*-carborane wheels have BH at every intersection except the black pointed vertices, which represent C and CH positions, *ipso* and *para*, respectively, relative to the alkyne. (Right) Structure of the second generation motorized nanocar 2. Synthesis of 2 involved assembling the rotor (red), the stator (blue), and the axles (green) that bear carborane wheels.

of the first generation nanocar greatly enhanced the rotation rate by replacing the thiopyran rotor with a cyclopentanylidene rotor.[16,17] This increased the rotation rate by 10^{12}, producing a MHz unidirectional molecular motor. Accordingly, we designed the second generation motorized nanocar **2** (Figure 1). Here, we report the synthesis of **2** and its imaging by STM at low temperature. This is a powerful method for the investigation of single nanomachines on a surface[18] because thermal motion is suppressed. Moreover, it permits manipulation of single functional molecules by inducing internal changes,[19] lateral motion on a surface,[20] or chemical modifications.[21] Furthermore, the changes within one and the same molecule upon light illumination from outside the ultrahigh vacuum chamber can be studied.[22] The molecular functions can thus be probed at the single-molecule level with the complete information of the atomic-scale environment of each individual molecule.

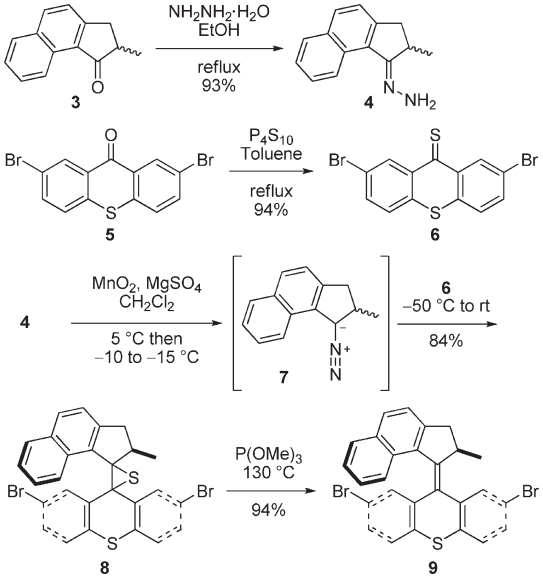

Scheme 1. Synthesis of molecular motor 9.

RESULTS AND DISCUSSION

Our plan to synthesize nanocar **2** involved a modular approach in which the coupling of the axles and the stator represent the last step. According to Scheme 1, heating ketone **3** to reflux in an ethanol and hydrazine solution produced the rotor, hydrazone **4**.[23] The conversion of ketone **5** into thione **6** was improved by decreasing both the concentration and the reaction time from that in the published procedure.[12] The key step, generation of the sterically hindered double bond between the rotor and the stator, utilized the Barton–Kellogg coupling. Hydrazone **4** was oxidized to the unstable diazo intermediate **7** using manganese dioxide with careful temperature control. The inorganic residue was removed by filtration in a Schlenk-type setup. Thione **6** was added portionwise to the deep-purple filtrate. A [2 + 3] cycloaddition occurred, and evolution of nitrogen gas indicated the formation of episulfide **8**. The white solid episulfide **8** was then treated with trimethyl phosphite in a screw-capped tube at 130 °C to afford molecular motor **9** in both chiral forms. As we plan to investigate individual molecules on surfaces, it was unnecessary to resolve the enantiomers.

We confirmed the structural integrity of key intermediate motor **9** (Scheme 1) using NMR techniques. All of the protons of motor **9** were unambiguously assigned with the assistance of correlation spectroscopy (COSY), nuclear Overhauser enhancement spectroscopy (NOESY), distortionless enhancement by polarization transfer spectroscopy (DEPT), heteronuclear single-quantum correlation spectroscopy (HSQC), and heteronuclear multiple-bond correlation spectroscopy (HMBC) experiments as detailed by the nuclear Overhauser enhancement (NOE) correlation arrows in Figure 2a and the accompanying spectrum.

The chemical shift difference steadily decreases between corresponding protons on the two benzene

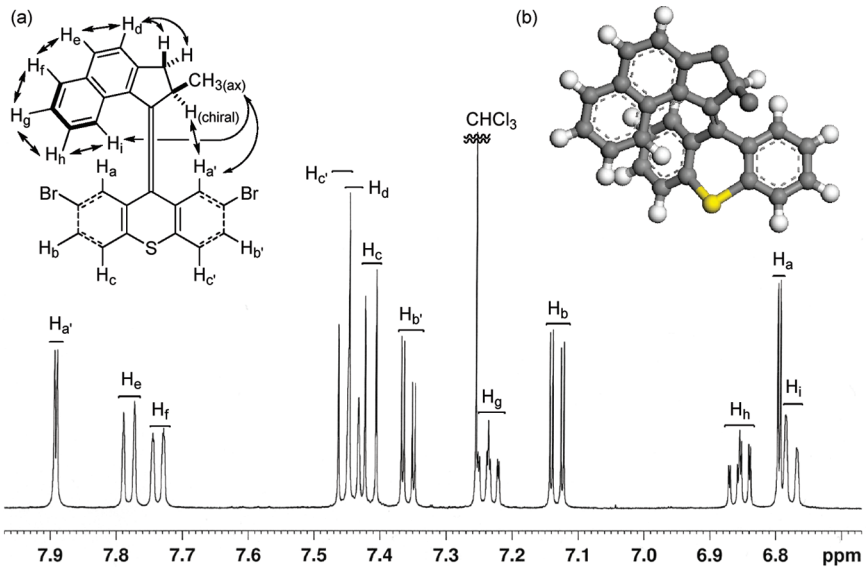

Figure 2. (a) Partial ^{1}H NMR (500 MHz, $CDCl_3$) at 295 K of molecular motor 9. Selected NOE signals (double-headed arrows) were used to assign individual proton signals in the aromatic region as indicated in the top left structure. (b) Ball-and-stick model of the energy-minimized *R*-isomer of motor 9 (Materials Studio with forcite force field).

rings on the thioxanthene stator: $\Delta\delta$ (H_a, $H_{a'}$) = 1.10 ppm, $\Delta\delta$ (H_b, $H_{b'}$) = 0.23 ppm, and $\Delta\delta$ (H_c, $H_{c'}$) = 0.04 ppm, consistent with the steadily increasing distance of these pairs from the rotor. The chemical shifts of protons H_h, H_i, and H_a reflect the shielding effect caused by the presence of an aromatic ring directly above H_a or directly below H_h and H_i. Compared to H_h and H_i, the most shielded aromatic protons in precursors **3** and **4** are at δ 7.49−7.52[24] and δ 7.32−7.38,[23] respectively; compared to H_a, the most shielded aromatic protons in precursors **5** and **6** are at δ 7.43[25] and δ 7.46,[12] respectively. Interestingly, no NOE signals were found between H_a, H_i and H_a, H_h; this can be rationalized by the helical structure of the rotor, as seen in Figure 2b. Proton H_i exhibits the most complex line shape among the aromatic protons (more clearly shown in the Supporting Information); not only does H_i couple to H_f, H_g, and H_h but also the COSY experiment reveals coupling between H_i and each of the CH_2 protons.

We attempted the final assembly (Scheme 2, route I) of nanocar **2** using a method similar to our synthesis of nanocar **1**.[12] However, the subtle structural differences between the motors produced a remarkable difference in reactivities. Sonogashira coupling between trimethylsilylacetylene (TMSA) and **9** using conventional $Pd(PPh_3)_2Cl_2$ and CuI conditions did not afford the desired bis-coupled product, probably due to steric hindrance between the bromine atoms and the naphthalene rotor unit. Thus, a more reactive catalyst developed by Fu and co-workers[26] was used, but the result was disappointing because of a high degree of decomposition. Therefore, the more stable alkyne source, triisopropylsilylacetylene (TIPSA), was reacted with dibromide **9**. In a mixture of 6:1 NEt_3/THF as base

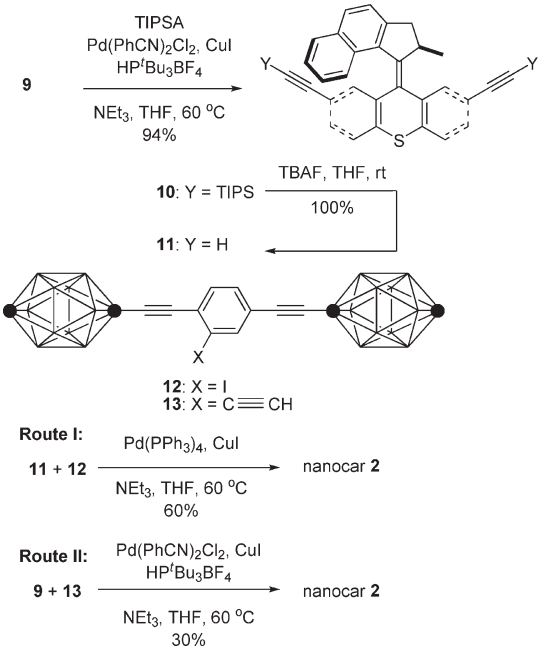

Scheme 2. Synthesis of the second generation motorized nanocar 2 through two different approaches.

and solvent, the Sonogashira coupling smoothly gave TIPS-protected bisacetylene motor **10** in excellent yield. Compound **10** was deprotected using TBAF, producing dialkyne **11** in quantitative yield. Sonogashira coupling was used between dialkyne **11** and previously reported axle **12**[12] using $Pd(PPh_3)_4$ and CuI as catalysts to produced nanocar **2** in moderate yield. Therefore, we tried a more convergent synthetic pathway (Scheme 2, route II) by utilizing Sonogashira coupling between motor **9** and alkynylated axle **13**[6] by applying conditions analogous to those for the

synthesis of **10**. Motorized nanocar **2** was thus obtained but in lower overall yield than that obtained from route I.

We evaporated nanocar **2** thermally under ultrahigh vacuum conditions onto a clean Cu(111) surface with large, flat terraces and imaged the surface by low-temperature STM. If very low coverages are chosen, we find clean terraces and all molecules adsorbed at the step edges. This shows that the molecules, although being rather large and thus exhibiting significant interaction with the metal surface, are mobile at room temperature and diffuse to the step edges where they are bound more strongly than on a terrace. However, for a clear insight into molecular motion upon external stimuli, as STM manipulation or light illumination, adsorption of the molecules on a flat terrace is preferred because the environment is equal for all molecules and the diffusion barrier is lower. Hence, we have deposited larger coverages of molecules onto the surface to saturate the step edges and force the molecules to adsorb on the terraces. On the resulting surface (Figure 3a), single molecules are indeed found (as marked by circles). In addition to them, we also observe a significant number of small protrusions that might represent single carborane groups, which are either present in small amounts in the molecular substance, but due to their small weight appear in large numbers on the surface,[27] or result from molecular fragmentation during deposition. Furthermore, islands are present on the terraces, which contain nanocar **2** molecules and unidentified small species in a disordered fashion.

When studying in detail the single molecules on a clean terrace (Figure 3b,d), we find characteristic appearances that consist of five lobes, four from the wheels and one from the motor. As some of the bonds in the chassis of the nanocar are rotatable, the two axles of the molecule can be either crossed (Figure 3b,c) or parallel (Figure 3d,e). When comparing the measured dimensions with those from gas phase simulations, there is a particularly good agreement for the lengths of the axles (d_1 and d_3), whereas the distances between opposite carborane wheels (d_2 and d_4) are slightly off. We assign this effect to the intramolecular flexibility of the central motor. Hence, the molecular appearance in STM images and the measured dimensions reveal that intact nanocar **2** molecules are present on the surface. The first illumination experiments were done at a wavelength of 248 nm and exposure times of up to 45 min at a pulse rate of 10 Hz (incidence angle of about 70° from the surface normal). However, no lateral motion of the molecules could be induced, monitoring the exactly same surface area that was imaged before the light exposure. Note furthermore that lateral motion could not be induced by STM manipulation, that is, using the STM tip, in our first experiments, which indicates a rather strong molecule–surface interaction.

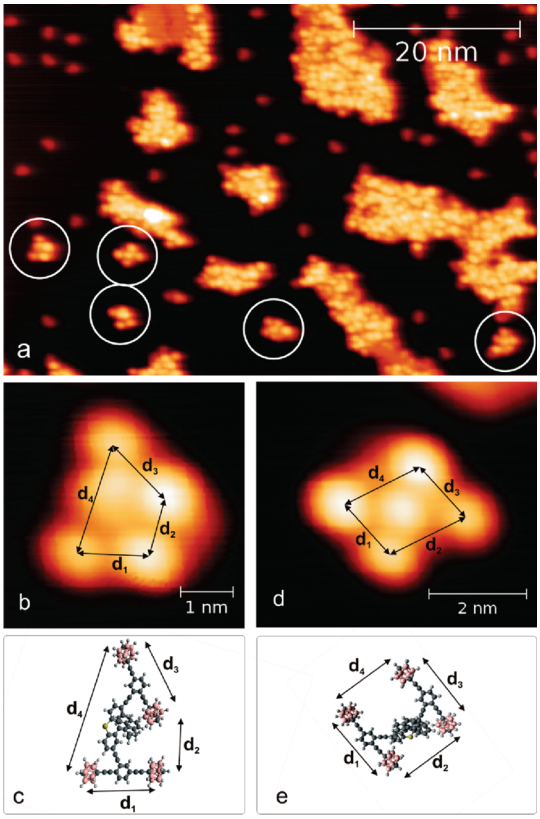

Figure 3. STM images of nanocar 2 on Cu(111) and calculated gas phase structures (HyperChem 7 software). (a) Overview image of the surface (white circles indicate wheels and motors of single molecules, partially adsorbed at defects). Intramolecular dimensions, determined from STM images, are compared with the calculated gas phase structure. Crossed axes: d_1 = 1.33 nm in the STM image (b) (and 1.38 nm in the calculation (c)), d_2 = 1.10 nm (1.07 nm), d_3 = 1.39 nm (1.38 nm), d_4 = 2.15 nm (2.29 nm). Parallel axles (d,e): d_1 = 1.38 nm in the STM image (d) (and 1.38 nm in the calculation (e)), d_2 = 1.65 nm (1.42 nm), d_3 = 1.37 nm (1.38 nm), d_4 = 1.70 nm (1.51 nm).

CONCLUSION

In this work, we successfully synthesized and did preliminary STM imaging of second generation nanocar **2**. We imaged single molecules after deposition onto Cu(111), revealing that—despite their size and complexity—it is possible to transfer them intact onto a surface under ultrahigh vacuum conditions. Their appearance in the STM images is in good agreement with the molecular dimensions in the gas phase, and according to their chemical structure, two typical conformations are identified. However, lateral motion on the surface, in particular, by activating the molecular motor, could not be achieved in our initial experiments. Future experiments will focus on this challenge by using different metallic and nonmetallic surfaces to modify the molecule–surface coupling in a controlled

way. As a complementary imaging method, SMFM has been used to monitor rolling motion of many fluorescent nanocars synthesized in our group.[7,8] We are evaluating the possibility of making inherently fluorescent motorized nanocars that have excitations and emission at a usable region.

METHODS

Experimental Details of NMR Analyses. A Bruker Avance-500 spectrometer using a broad band observe probe with a *z*-axis gradient coil and the standard Bruker pulse programs indicated were used for these analyses. ^{1}H (zg30): 30° pulse, 13.11 s FID, 5 s relaxation delay, 16 scans, no line broadening. COSY (cosygpqf): 2048 increments for an F_1 digital resolution = 0.0049 ppm, 12 scans/increment, FID acquisition time = 0.41 s for an F_2 digital resolution = 0.0024 ppm, relaxation delay = 1.5 s. NOE (noesygpph), mixing time = 1 s, 2048 increments for an F_1 digital resolution = 0.0049 ppm, 4 scans/increment, FID acquisition time = 0.41 s for an F_2 digital resolution = 0.0024 ppm, relaxation delay = 1 s. A second NOE experiment with a mixing time of 1.75 s and 8 scans/increment did not yield any additional information. ^{13}C (zgpg): 90° pulse, 6.60 s FID, 5 s relaxation delay, 664 scans, 0.10 Hz line broadening. DEPT-135 ^{13}C (dept135): optimized for $^1J_{CH}$ = 145 Hz, 6.60 s FID, 5 s relaxation delay, 128 scans, 0.10 Hz line broadening. ^{1}H−^{13}C HSQC (hsqcetgp): optimized for $^1J_{CH}$ = 145 Hz, 2048 increments for ^{13}C digital resolution = 0.069 ppm (zero-filled once), 16 scans/increment. The ^{13}C digital resolution was just enough to enable pairwise ^{1}H/^{13}C assignments for the ^{13}C signals at δ 129.109, 129.143, and 129.190. ^{1}H−^{13}C HMBC (hmbcgplpndqf): optimized for $^1J_{CH}$ = 145 Hz, optimized for long-range J_{CH} = 6.25 Hz, 2048 increments for ^{13}C digital resolution = 0.077 ppm (zero-filled once), 48 scans/increment.

Synthesis of Nanocar 2. Route I: An oven-dried 10 mL Schlenk tube equipped with a stir bar was charged with molecular motor **11** (45 mg, 0.106 mmol), axle **12** (128 mg, 0.238 mmol), $Pd(PPh_3)_4$ (9.8 mg, 8.5 μmol), and CuI (3.3 mg, 17 μmol) to which were added NEt_3 (0.15 mL) and THF (1 mL). The reaction mixture was stirred at 60 °C for 16 h, and then it was cooled to room temperature. The mixture was quenched with saturated NH_4Cl (20 mL) and extracted with dichloromethane (30 mL). The organic phase was washed with water (30 mL), dried over anhydrous $MgSO_4$, filtered, and the filtrate was concentrated under vacuum. The crude product was purified by column chromatography (silica gel, 8% CH_2Cl_2 in hexanes) to yield **2** as a pale yellow solid (78 mg, 60%). Route II: Inside a glovebox, a 20 mL screw-capped tube equipped with a stir bar was charged with molecular motor **9** (26 mg, 49 μmol), axle **13** (63 mg, 0.146 mmol), $Pd(PhCN)_2Cl_2$ (4 mg, 10 μmol), $HP^tBu_3BF_4$ (5.7 mg, 20 μmol), CuI (4 mg, 20 μmol), NEt_3 (3 mL), and THF (1 mL). The reaction mixture was stirred at 60 °C for 16 h, and then it was cooled to room temperature. The mixture was quenched with saturated NH_4Cl (20 mL) and extracted with dichloromethane (30 mL). The organic phase was washed with water (30 mL), dried over anhydrous $MgSO_4$, filtered, and the filtrate was concentrated under vacuum. The crude product was purified by column chromatography (silica gel, 5% CH_2Cl_2 in hexanes) to yield **2** as a pale yellow solid (18 mg, 30%): mp >200 °C (decomp); FTIR (neat) 3060, 2956, 2924, 2866, 2846, 2610, 2208, 1594, 1488, 1454, 1140, 1062 cm^{-1}; ^{1}H NMR (500 MHz, CD_2Cl_2) δ 8.03 (d, J = 1.7 Hz, 1H), 7.81 (d, J = 8.2 Hz, 1H), 7.73 (d, J = 8.2 Hz, 1H), 7.70−7.65 (m, 2H), 7.53 (d, J = 8.2 Hz, 1H), 7.48−7.45 (m, 2H), 7.28−7.25 (m, 2H), 7.23 (ddd, J_1 = 7.4 Hz, J_2 = 7.2 Hz, J_3 = 1.5 Hz, 1H), 7.18 (dd, J_1 = 8.1 Hz, J_2 = 1.7 Hz, 1H), 7.14−7.10 (m, 2H), 7.06 (dd, J_1 = 8.0 Hz, J_2 = 1.8 Hz, 1H), 6.94 (dd, J_1 = 2.0 Hz, J_2 = 0.4 Hz, 1H), 6.93−6.87 (m, 2H), 4.34 (qd, J_1 = 6.8 Hz, J_2 = 6.3 Hz, 1H), 3.84 (dd, J_1 = 15.6 Hz, J_2 = 6.3 Hz, 1H), 3.20−1.60 (br m, 45H), 0.86 (d, J = 6.8 Hz, 3H); ^{13}C NMR (125 MHz, CD_2Cl_2) δ 148.3, 147.4, 140.9, 138.5, 137.5, 137.2, 135.6, 135.4, 134.8, 133.7, 132.8, 132.5, 132.1, 131.52, 131.50, 131.22, 131.19, 130.3, 129.9, 129.3, 128.6, 128.5, 128.3, 127.2, 126.9, 126.8, 126.3, 125.6, 124.9, 124.5, 124.4, 124.1, 122.6, 122.3, 121.5, 121.3, 94.7, 94.3, 91.7, 91.5, 88.4, 88.2, 87.5, 86.8, 78.4, 78.3, 78.2, 78.0, 69.7 (br), 69.6 (br), 61.2 (br), 40.4, 38.6, 19.9; HRMS (APCI) *m/z* calcd for $[M + H]^+$ $C_{59}H_{69}{}^{10}B_7{}^{11}B_{33}S$ 1242.9096, found 1242.9124.

Motorized Nanocar 2 STM Imaging Procedure. The scanning tunneling microscopy (STM) experiments were performed in an ultrahigh vacuum (UHV) chamber with a base pressure of 10^{-10} mbar. The Cu(111) surface was cleaned through repeated cycles of Ar^+ sputtering and annealing at 400 °C. The molecules were thermally evaporated from a Knudsen cell, held at about 300 °C, onto the Cu(111) surface (at 50 °C). The STM images were taken in an Omicron low-temperature (LT) STM working at 5.7 K using a W tip. All images have been taken using a tip bias of −1 V and a tunneling current of 1 pA. Gas phase calculations were performed using the HyperChem 7 software.

Acknowledgment. We thank the NSF NIRT (ECCS-0708765), NSF Nanocars (CHE-1007483), the NSF Penn State MRSEC and Center for Nanoscale Science, and the German Science Foundation DFG (through SFB 658) and the European Project ARTIST for providing financial support. We also thank Drs. I. Chester of FAR Research, Inc., and R. Awartari of Petra Research, Inc., for providing trimethylsilylacetylene.

Supporting Information Available: Synthetic procedures and spectra of new compounds, and NMR analyses of motor **9**. This material is available free of charge *via* the Internet at http://pubs.acs.org.

REFERENCES AND NOTES

1. Chiang, P.-T.; Cheng, P.-N.; Lin, C.-C.; Liu, Y.-H.; Lai, C.-C.; Peng, S.-H.; Chiu, S.-H. A Macrocycle/Molecular-Clip Complex That Functions as a Quadruply Controllable Molecular Switch. *Chem.—Eur. J.* **2006**, *12*, 865–876.
2. Badjic, J. D.; Balzani, V.; Credi, A.; Silvi, S.; Stoddart, J. F. A Molecular Elevator. *Science* **2004**, *303*, 1845–1849.
3. Chuang, C.-J.; Li, W.-S.; Lai, C.-C.; Liu, Y.-H.; Peng, S.-H.; Chao, I.; Chiu, S.-H. A Molecular Cage-Based [2]Rotaxane That Behaves as a Molecular Muscle. *Org. Lett.* **2009**, *11*, 385–388.
4. Shirai, Y.; Morin, J.-F.; Sasaki, T.; Guerrero, J. M.; Tour, J. M. Recent Progress on Nanovehicles. *Chem. Soc. Rev.* **2006**, *35*, 1043–1055.
5. Vives, G.; Tour, J. M. Synthesis of Single-Molecule Nanocars. *Acc. Chem. Res.* **2009**, *42*, 473–487.
6. Villagómez, C. J.; Sasaki, T.; Tour, J. M.; Grill, L. Bottom-up Assembly of Molecular Wagons on Surface. *J. Am. Chem. Soc.* **2010**, *132*, 16848–16854.
7. Khatua, S.; Guerrero, J. M.; Claytor, K.; Vives, G.; Kolomeisky, A. B.; Tour, J. M.; Link, S. Micrometer-Scale Translation and Monitoring of Individual Nanocars on Glass. *ACS Nano* **2009**, *3*, 351–356.
8. Khatua, S.; Godoy, J.; Tour, J. M.; Link, S. Influence of the Substrate on the Mobility of Individual Nanocars. *J. Phys. Chem. Lett.* **2010**, *1*, 3288–3291.
9. Shirai, Y.; Osgood, A. J.; Zhao, Y.; Kelly, K. F.; Tour, J. M. Directional Control in Thermally Driven Single-Molecule Nanocars. *Nano Lett.* **2005**, *5*, 2330–2334.
10. Shirai, Y.; Osgood, A. J.; Zhao, Y.; Yao, Y.; Saudan, L.; Yang, H.; Chiu, Y.-H.; Alemany, L. B.; Sasaki, T.; Morin, J.-F.; *et al.* Surface-Rolling Molecules. *J. Am. Chem. Soc.* **2006**, *128*, 4854–4864.
11. Godoy, J.; Vives, G.; Tour, J. M. Toward Chemical Propulsion: Synthesis of ROMP-Propelled Nanocars. *ACS Nano* **2011**, *5*, 85–90.
12. Morin, J.-F.; Shirai, Y.; Tour, J. M. En Route to a Motorized Nanocar. *Org. Lett.* **2006**, *8*, 1713–1716.
13. Sasaki, T.; Tour, J. T. Synthesis of a New Photoactive Nanovehicle: A Nanoworm. *Org. Lett.* **2008**, *10*, 897–900.

14. Shirai, Y.; Sasaki, T.; Guerrero, J. M.; Yu, B.-C.; Hodge, P.; Tour, J. M. Synthesis and Photoisomerization of Fullerene–and Oligo(phenylene ethynylene)–Azobenzene Derivatives. *ACS Nano* **2008**, *2*, 97–106.
15. Koumura, N.; Geertsema, E. M.; van Gelder, M. B.; Meetsma, A.; Feringa, B. L. Second Generation Light-Driven Molecular Motors. Unidirectional Rotation Controlled by a Single Stereogenic Center with Near-Perfect Photoequilibria and Acceleration of the Speed of Rotation by Structural Modification. *J. Am. Chem. Soc.* **2002**, *124*, 5037–5051.
16. Klok, M.; Boyle, N.; Pryce, M. T.; Meetsma, A.; Browne, W. R.; Feringa, B. L. MHz Unidirectional Rotation of Molecular Rotary Motors. *J. Am. Chem. Soc.* **2008**, *130*, 10484–10485.
17. Kulago, A. A.; Mes, E. M.; Klok, M.; Meetsma, A.; Brouwer, A. M.; Feringa, B. L. Ultrafast Light-Driven Nanomotors Based on an Acridane Stator. *J. Org. Chem.* **2010**, *75*, 666–679.
18. Grill, L.; Rieder, K.-H.; Moresco, F.; Jimenez-Bueno, G.; Wang, C.; Rapenne, G.; Joachim, C. Imaging of a Molecular Wheelbarrow by Scanning Tunneling Microscopy. *Surf. Sci.* **2005**, *584*, L153–L158.
19. Grill, L.; Rieder, K.-H.; Moresco, F.; Stojkovic, S.; Gourdon, A.; Joachim, C. Exploring the Interatomic Forces between Tip and Single Molecules during STM Manipulation. *Nano Lett.* **2006**, *6*, 2685–2689.
20. Grill, L.; Rieder, K.-H.; Moresco, F.; Rapenne, G.; Stojkovic, S.; Bouju, X.; Joachim, C. Rolling a Single Molecular Wheel at the Atomic Scale. *Nat. Nanotechnol.* **2007**, *2*, 95–98.
21. Hla, S.-W.; Bartels, L.; Meyer, G.; Rieder, K.-H. Inducing All Steps of a Chemical Reaction with the Scanning Tunneling Microscope Tip: Towards Single Molecule Engineering. *Phys. Rev. Lett.* **2000**, *85*, 2777–2780.
22. Comstock, M. J.; Levy, N.; Kirakosian, A.; Cho, J.; Lauterwasser, F.; Harvey, J. H.; Strubbe, D. A.; Frechet, J. M. J.; Trauner, D.; Louie, S. G.; *et al.* Reversible Photomechanical Switching of Individual Engineered Molecules at a Metallic Surface. *Phys. Rev. Lett.* **2007**, *99*, 038301.
23. ter Wiel, M. K. J.; Vicario, J.; Davey, S. G.; Meetsma, A.; Feringa, B. L. New Procedure for the Preparation of Highly Sterically Hindered Alkenes Using a Hypervalent Iodine Reagent. *Org. Biomol. Chem.* **2005**, *3*, 28–30.
24. ter Wiel, M. K. J.; van Delden, R. A.; Meetsma, A.; Feringa, B. L. Increased Speed of Rotation for the Smallest Light-Driven Molecular Motor. *J. Am. Chem. Soc.* **2003**, *125*, 15076–15086.
25. Coleman, M. P.; Boyd, M. K. S-Pixyl Analogues as Photocleavable Protecting Groups for Nucleosides. *J. Org. Chem.* **2002**, *67*, 7641–7648.
26. Hundertmark, T.; Littke, A. F.; Buchwald, S. L.; Fu, G. C. $Pd(PhCN)_2Cl_2/P(t\text{-}Bu)_3$: A Versatile Catalyst for Sonogashira Reactions of Aryl Bromides at Room Temperature. *Org. Lett.* **2000**, *2*, 1729–1731.
27. Rapenne, G.; Grill, L.; Zambelli, T.; Stojkovic, S. M.; Ample, F.; Moresco, F.; Joachim, C. Launching and Landing Single Molecular Wheelbarrows on a Cu(100) Surface. *Chem. Phys. Lett.* **2006**, *431*, 219–222.